Using Radiomics-based Modeling to Predict Individual Progression From Mild Cognitive Impairment to Alzheimer's Disease

Jiehui Jiang (jiangjiehui@shu.edu.cn)
Shanghai University https://orcid.org/0000-0003-4948-3683
Xiaoming Sun
Shanghai University
Ian Alberts
Inselspital University Hospital Bern: Inselspital Universitatsspital Bern
Min Wang
Shanghai University
Axel Rominger
Inselspital University Hospital Bern: Inselspital Universitatsspital Bern
Chuantao Zuo
Huashan Hospital Fudan University
Ying Han
Beijing Xuanwu Hospital: Xuanwu Hospital
Kuangyu Shi
Inselspital University Hospital Bern: Inselspital Universitatsspital Bern

Research Article

Keywords: Radiomic-based predictive model, Alzheimer's disease, mild cognitive impairment, radiomics, Cox model

Posted Date: August 6th, 2021

DOI: https://doi.org/10.21203/rs.3.rs-775291/v1

Abstract

Background: Predicting the risk of disease progression from mild cognitive impairment (MCI) to Alzheimer's disease (AD) has important clinical significance. This study aims at providing a personalized MCI-to-AD conversion prediction *via* radiomics-based predictive modeling (RPM) with multicentre ^{18}F-Fluorodeoxyglucose positron emission tomography (FDG PET) data.

Method: Three cohorts of 18F-FDG PET data and neuropsychological assessments were gathered from patients examined at Huashan Hospital (n=22), Xuanwu Hospital (n=80), and from the Alzheimer's Disease Neuroimaging Initiative (ADNI) database (n=355). Of these, amyloid images were selected for the ADNI and Xuanwu cohorts. First, 430 radiomic features were extracted from the 80 regions of interest (ROIs) for all PET images. These features were then concatenated for feature selection and an RPM model was constructed on the ADNI dataset. In addition, we used clinical scale data to establish a clinical Cox model, and a combined model for comparison. Afterwards, the images from Huashan Hospital were used to validate the stability and reliability of RPM, and the images from Xuanwu Hospital were used to explore the differences of biomarkers at different cognitive stages. Finally, correlation analysis was conducted between the radiomic biomarkers, neuropsychological assessments, and amyloid burden.

Results: Experimental results show that the predictive performance of the PET-modal cox model was better than clinical cox model. In the two test data sets, the C index of PET model is 0.75 and 0.73, respectively; The C index of clinical model is 0.68. Moreover, most crucial image biomarkers had significant differences at different cognitive stages, and were significantly correlated with cognitive ability and the amyloid global level standardized uptake value ratio.

Conclusion: The preliminary results demonstrated that the developed RPM approach has the potential to monitor the progress in high-risk populations with AD.

1 Introduction

Alzheimer's disease (AD) is the most common neurodegenerative disease, and its main manifestations include abnormal deposition of pathological proteins (such as β-amyloid and tau-neurofibrillary tangles) resulting in neurological dysfunction [1, 2]. Mild cognitive impairment (MCI) is considered a prodromal-stage with high-risk for the individual's ultimate conversion to AD. However, the neuropathological substrates of MCI are heterogeneous, many MCI patients remain stable, or even return to a normal state, while other patients progress to AD [3, 4]. Therefore, it is of great clinical significance to identify the risk factors and biomarkers for predicting the progression from MCI to AD.

Neuroimaging plays an increasingly important role in the clinical diagnosis of AD, such as magnetic resonance imaging (MRI) and positron emission tomography (PET), which has been widely used in AD studies [1, 5, 6]. Several potential imaging biomarkers are regarded as effective predictors of early AD prediction, such as brain atrophy and glucose hypometabolism [7, 8]. Furthermore, previous studies have found that ^{18}F-Fluorodeoxyglucose positron emission tomography (^{18}F-FDG PET) is a neuroimaging scan

that significantly advances the clinical diagnostic value in predicting MCI progression [9–11]. However, in most cases, the standard uptake value (SUV) is usually used as a biomarker to represent metabolic information, and it is not enough to provide diagnostic support. Therefore, better biomarkers and predictive models are needed to assist for MCI-to-AD conversion prediction.

Radiomics aims to extract quantitative data by means of high-throughput mining of image features and to establish relevant statistical models which might inform a personalized medicine approach [12, 13]. For example, the high dimensional image characteristic, quantitative 'Coarseness' value can be used to represent the spatial change rate level of voxel intensity in the brain (as shown in the Fig. 1), whereas the SUVs in both brain regions may be same. Similarly, high-throughput quantitative interpretable features are used to build models after data mining. Radiomics has also been applied to early diagnosis of AD prediction research, which indicates that radiomics-based predictive modeling (RPM), a data-driven method for extracting and summarizing the most relevant features from neuroimaging data in order to construct predictive models, has potential to perform individual-level predictions of MCI progression [14–19].

Moreover, one challenge is that the stability and reproducibility of radiomic features have not been fully investigtated, with few studies reporting multi-center data. Considering the shortcomings of existing studies on radiomics analysis, the primary objective of this work was to investigate the feasibility of RPM prediction of MCI progression using multi-center FDG PET images. We hypothesize that imaging biomarkers of MCI progression derived from RPM and PET data can be used to predict individualized progression risk in MCI patients.

2 Materials And Methods

2.1 Subjects

Three cohorts of patients with PET imaging data were collected, including 355 patients from the Alzheimer Disease Neuroimaging Initiative (ADNI) database (adni.loni.usc.edu, Cohort I), 22 patients from Huashan hospital (Cohort II), and 80 patients from Xuanwu hospital (Cohort III). Of these, subjects with amyloid-PET (Florbetapir F-18 [AV45]) scanning were selected for the Cohort I and III. This study was approved by institutional review boards of ADNI, Huashan, and Xuanwu hospital, and written informed consent was obtained from all participants or authorized representatives.

The inclusion criteria for data collection were as follows: 1) Subjects had both MRI and FDG PET scans and neuropsychological assessments (mini-mental state examination, MMSE) at baseline. 2) For MCI non-converters, patients did not convert to AD during the three-year follow-up period; for MCI converters, who converted to AD within three-year. 3) Participants with a bidirectional change of diagnosis (MCI to AD, and back to MCI) within the follow-up period were excluded. 4) SCD was defined by the research criteria for pre-MCI (SCD) proposed by Jessen et al in 2014 [20]; both MCI and AD dementia patients were included as cognitive impairment (CI) group.

2.2 Acquisition protocol

All subjects in this study were scanned by FDG PET and structural T1 MRI imaging. For detailed information on data acquisition of Cohort I, please refer to the description in the imaging protocol column of the ADNI database (http://adni.loni.usc.edu/). MRI data in Cohort II were acquired with a 3T MR750 scanner manufactured by General Electric Company. All subjects in Cohort II performed FDG PET scanning in 3D mode using a Siemens Biograph 64 HD PET/CT at resting state. All subjects fasted for at least 6 hours before the examination. After intravenous injection of 185 MBq FDG, subjects underwent a PET scan after resting for 45 minutes. MRI data of in Cohort III were acquired using a 3T TOF PET/MR scanner produced by General Electric Company. FDG PET data in Cohort III was performed in a 3D mode. Each subject was instructed to fast for at least 6 hours before the FDG PET scan. Approximately 40 minutes after intravenous injection of 3.7 MB/kg of ^{18}F-FDG, a 35-minute dynamic scan was performed.

2.3 Data pre-processing

Data preprocessing for both PET and MRI images was done by using Statistical Parametric Mapping 12 (SPM12, the Wellcome Department of Neurology, London U.K.) implemented in Matlab 2016b (Mathworks Inc.). First, original FDG PET image for each subject was registered with corresponding structural MRI image. Then, MRI images were segmented into gray matter (GM), white matter (WM), and cerebrospinal fluid (CSF) tissue probability maps using the unified segmentation method. The registered PET image was spatially normalized to the MNI space using the transformation parameters. Finally, the normalized PET images were smoothed using an isotropic Gaussian kernel of 8 mm to increase signal-to-noise ratios. Notably, all FDG PET images were underwent count normalization using the global cortical uptake to increase individual metabolic differences, as the mean cortical SUVR representing amyloid β level.

2.4 Radiomics-based predictive modelling analysis

In this study, we implemented RPM method to develop predictive models of brain-behavior relationships from glucose metabolic data. RPM method included the following steps: 1) radiomics feature extraction, 2) radiomics feature summarization, 3) model building and assessment, and 4) validation of crucial features.

Feature extraction

To obtain more detailed features, 80 cortical regions from the automated anatomical labeling (AAL) atlas were used as ROIs. We extracted 430 radiomics features from each ROIs for FDG PET data. In brief, the most basic features in each ROIs include two parts: first-order intensity features (n = 3) and texture features (n = 40). We extracted features under the combination of different wavelet filter weights (5 levels) and quantization of gray levels (2 levels), and the total number of features per ROIs was 430 ((3 + 40) * 5 * 2 = 430). The details of these features could obtain in **supplement**.

Feature summarization

The 10-fold cross-validation and Z-normalization strategies were implemented in Cohort I. To reduce the dimension of features and solve the over-fitting problem, three feature selection methods were performed separately for training data in Cohort I. The feature selection steps were as follows: 1) Feature stability analysis: the stable features with Cronbach's alpha coefficient greater than 0.75 were selected in longitudinal HC data in Cohort I. 2) Statistical test: *t*-test and rank sum *t*-test were used to identify the features with significant differences ($P < 0.01$) [21]. 3) Least absolute shrinkage and selection operator (LASSO).

Model construction and assessment

The Cox model was constructed using radiomics features from FDG PET. Ten-fold cross-validation was used to evaluate the prediction performance. Cox model was constructed during the training phase while selecting typical features. The clinical outcome was whether MCI subject was converted to AD. Time of outcome appearance was the interval between the baseline time and the endpoint. The Cox model was used in the test dataset to calculate the prognostic index (PI) for each subject. PI was a linear combination of the selected feature and its coefficient. The prediction performance of the model was evaluated using Harrell's consistency coefficient (C-index). The C-index of the test dataset was calculated by PI. In addition, we also counted the number of times each feature participated in model construction. It is worth noting that the 10-fold cross-validation was also repeated 20 times, and the conserved features were also identified. These conserved features were used for further analysis.

Clinical Cox model was also constructed using available clinical variables (age, gender, education, and MMSE) to compare the predictive performance with RPM method. Cohort II data was used for external validation of the predictive model derived from RPM method.

Validation of crucial features

To further explore the relationship between conserved features and Neuropsychiatric assessments at different cognitive stages, partial correlation coefficients were calculated between the features neuropsychological assessments, and amyloid burden in individual subjects, combining MCI converters and MCI non-converters in Cohort I and combining SCD and CI subjects in Cohort III. The effects of age, gender and education were controlled. We also evaluated the differences in the identified features between HC, MCI-nc and MCI-c in Cohort I and HC, SCD and CI in Cohort III.

To further study the prediction performance of key features of important brain regions, we used features in the brain regions related to MMSE and amyloid β level as predictors to construct Cox models, respectively. The prognostic index of each subject was calculated according to the corresponding model, and then the individuals were stratified into high-risk and low-risk prognostic groups according to the median of prognostic index. Log-rank test was employed to examine the survival difference between different risk groups. We also combined these features to build a comprehensive Cox model and evaluated its performance for disease stratification.

As a comparison, the SUVR values of hippocampus, paracingulate gyrus and whole brain area as the feature were used to construct the SUVR Cox model. The process was the same as described above.

Statistical analysis

The group differences of clinical characteristics were assessed using two-sample t test, $\chi 2$ test, one-sample t test, or Tukey's test. Log-rank test was employed to examine the survival difference between different risk groups. P values were 2-tailed, and $P < 0.05$ was considered statistically significant. All statistical tests were performed using SPSS 24.0. Cox model were constructed in R (http://www.R-project.org/) employing the 'glmnet' and 'survival' packages [22–24].

3 Results

3.1 Subjects

Cohort I included 168 MCI converters, 187 MCI non-converters, and 94 healthy control (HC) subjects that had two follow-up visits from the ADNI database. Cohort II included 10 MCI converters and 12 MCI non-converters from Huashan Hospital. Cohort III included 33 HCs, 37 subjective cognitive decline (SCD) patients, and 10 cognitive impairment (CI) patients were from the Sino Longitudinal Study on Cognitive Decline project (SILCODE) project. Table 1 shows the demographic information for participants from each cohort.

Table 1
The clinical characteristics of all cohorts.

	Group	Sex (M/F)	Age (years) Mean ± SD	Education (year) Mean ± SD	MMSE Mean ± SD	Amyloid β level	Conversion time (months)
Cohort I	sMCI (*n* = 187)	109/78	72.1 ± 7.5	16.0 ± 2.6	28.0 ± 1.6	1.40 ± 0.22	0
	pMCI (*n* = 168)	95/73	74.0 ± 7.1	16.0 ± 2.6	26.5 ± 2.2	1.16 ± 0.20	14.1 ± 8.9
	P-value	0.74 [a]	0.018 [b]	0.91 [b]	< 0.001 [b]	< 0.001 [b]	/
	HC *(n = 94)*	48/46	72.8 ± 5.9	16.9 ± 2.4	29.2 ± 1.2	/	/
Cohort II	sMCI (*n* = 12)	5/7	64.3 ± 5.7	11.9 ± 2.9	26.9 ± 1.6	/	0
	pMCI (*n* = 10)	6/4	73.5 ± 4.1	13.7 ± 2.3	25.5 ± 2.2	/	25.5 ± 9.6
	P-value	0.39[a]	< 0.001 [b]	0.13 [b]	0.10 [b]	/	/
Cohort III	HC *(n = 33)*	15/18	67.1 4.5	13.1 ± 3.1	29.1 ± 1.4	/	
	SCD *(n = 37)*	8/29	66.0 4.6	12.8 ± 2.8	28.7 ± 1.7	1.15 ± 0.08	
	CI *(n = 10)*	5/5	65.9 7.2	12.7 ± 3.6	23.4 ± 3.4	1.30 ± 0.18	

3.2 Conserved features in Cox model

Radiomics analysis was used to extract 34 400 features from PET image of each subject. In the 10-fold cross-validation with 20 repetitions, we chose features that were included in the prediction model more than two thirds of the time. This resulted in 13 conserved features in the Cox model. The distribution of conserved features was as follows. The conserved features mainly came from the texture features of the cingulate cortex, hippocampus, parahippocampal gyrus, precuneus, and other temporoparietal regions. Table 2 lists the detailed information.

Table 2
Conserved features in the PET model

Rank	Times	Labelled number	Labelled region	Gray-Level	Feature name	Anatomical classification
1	196	64	SupraMarginal_R	32	SZHGE	Parietal
2	194	37	Hippocampus_L	32	GLV	Temporal
3	194	39	ParaHippocampal_L	64	Busyness	Temporal
4	185	68	Precuneus_R	64	Correlation	Parietal
5	181	33	Cingulum_Mid_L	32	ZP	Frontal
6	179	33	Cingulum_Mid_L	32	LZLGE	Frontal
7	176	67	Precuneus_L	32	ZSV	Parietal
8	157	8	Frontal_Mid_R	32	Skewness	Prefontal
9	144	18	Rolandic_Oper_R	64	Contrast	Frontalu
10	144	38	Hippocampus_R	64	Correlation	Temporal
11	144	68	Precuneus_R	64	Variance	Parietal
12	139	34	Cingulum_Mid_R	64	LZE	Frontal
13	137	85	Temporal_Mid_L	64	Contrast	Temporal

Note: Times: the number of times corresponding feature was selected in the 10-fold cross-validation with 20 repetitions, R: weights to bandpass sub-bands in wavelet filtering, Gray-Level: gray level quantization level, SZHGE: small zone high-gray-level emphasis, GLV: gray-level variance, ZP: zone percentage, LZLGE: large zone low gray-level emphasis, ZSV: zone-size variance, LZE: large zone emphasis.

3.3 PET model radiomics analysis predict progression MCI to AD

Three prediction models were constructed, including PET model, clinical model and combined model (Clinical + PET). This study compared the prediction performance of three models and identified the conserved features associated with MCI conversion in each model. The average C-index with multiple 10-fold cross-validation was used for the prediction performance evaluation. Generally, PET model was far superior to clinical model (0.753 (0.008) vs 0.684 (0.006) in Cohort I_Test, 0.734 (0.011) vs 0.685(0.006) in Cohort II). The combined model achieved a best predicition performance (0.766 (0.009) in Cohort I_Test, 0.798 (0.008) in Cohort II). Table 3 summarized the prediction performance evaluation of each model.

Table 3
The prediction performance of each model.

Model	Cohort I_Train	Cohort I_Test	Cohort II
Clinical	0.692 (0.0004)	0.684 (0.006)	0.685(0.006)
PET	0.871 (0.004)	0.753 (0.008)	0.734 (0.011)
Combined	0.884 (0.004)	0.766 (0.009)	0.798 (0.008)

3.4 Validation of crucial image features

Of these identified features, 11 showed significant correlations with the MMSE scores in Cohort I ($P < 0.05$) (Fig. 1A); 8 features showed significant correlations with the MMSE scores in Cohort III ($P < 0.05$) (Fig. 1A). 7 of the 13 features were significantly associated with the Aβ scores in Cohort I; 5 features were significantly associated with the Aβ scores in Cohort III ($P < 0.05$) (Fig. 1A). Figure 1B showed the correlation of a representative feature, zone percentage (ZP) from the left midcingulate area, with the MMSE score and Aβ score.

We explored differences of these identified features between healthy controls, MCI non-converters and MCI converters in Cohort I. The results showed that all 13 features were significantly different between MCI-c and MCI-nc groups; 10 features were significantly different between MCI-c and HC groups. We also compared the differences in these features at three cognitive stages in Cohort III. The results showed that 3 features were significantly different between CI and SCD groups; 5 features were significantly different between CI and HC groups; no differences were found between SCD and HC groups ($P < 0.05$, Tukey-Kramer correction) (Fig. 2A). Figure 2B demonstrated examples of feature distributions at different cognitive stages.

Figure 4 demonstrates the characteristics of the important brain areas found in the study and the brain area SUVR value and Kaplan-Meier survival curves of Cox model. In the model, 5 features were significant predictors. The quality of the Cox models was tested with the AIC test (model of crucial features: AIC value, 1542.74; model of SUVR values: AIC value, 1536.36). For the test dataset, model demonstrated good separation of groups with high and low risks of conversion to AD. The best stratification was reached with the prognostic index resulting from the PET model (model of crucial features, $P < 0.001$; model of SUVR values, $P = 0.010$).

4 Discussion

In this study, we designed a workflow for radiomics-based predictive modelling analysis using PET images. This workflow extracted a large number of quantitative features from PET images and identified dozens of crucial image markers. Based upon these markers we built and evaluated Cox regression models to predict the conversion outcomes results of MCI patients. Notably, as a multi centers research, we also validated our methodology using external PET data from the Huashan cohort, and explored the

correlation between crucial image markers and clinical information using images and data from the Xuanwu cohort. Further, the stratification effects of the predictors found in the study and the traditional SUVR values were compared.

As a result, a total of 34 400 quantitative features were extracted in 80 cortical regions for each modality of each subject. In this study, two Lasso-Cox models were constructed based on the source of the features, and the performance of the image-based prediction model was superior to the clinical model. This may be related to the low sensitivity and higher subjectivity of the neuropsychological scales [1]. The relatively low predictive performance of clinical models may be improved by further adding PET imaging information [25].Previous studies have shown that this information could also assist in MCI conversion prediction [25, 1]. On the external test data set in our study, the performance of the image-based prediction model is also better than that of the clinical model. These results further demonstrated that the methodology of this study was stable and reliable, proving the great potential of quantitative features from PET images to predict MCI conversion.

In this study, we considered all cortical regions as ROIs and extracted quantitative features from them. Surprisingly, our study found that most of the selected conserved features were located in areas consistent with previous studies, such as the hippocampus and parahippocampal gyrus in the temporal cortex, the precuneus and supramarginal gyrus in parietal, and the medial and paracingulate gyri in the frontal region and so on. In fact, previous studies have described these areas as important regions of structural changes and metabolic abnormalities associated with MCI conversion [26–28]. They were vulnerable target for AD pathology. Texture features extracted from these regions were more conducive to distinguishing MCI-converters from MCI non-converters. In addition to medial temporal lobe atrophy, atrophy of other brain regions also had additional predictive value for cognitive decline in MCI individuals, including the cingulate cortex and orbitofrontal cortex [29]. The decreased metabolism in the posterior cingulate gyrus and precuneus cortex was also one of the markers of progress from MCI to AD [5]. Quantitative features from these regions in PET model were also associated to MCI conversion. In conclusion, our study again confirmed that metabolic features from AD pathologically susceptible regions were more effective in predicting MCI conversion. Moreover, metabolic abnormalities in these areas could be better presented by high dimensional radiomic features.

Our study also explored the performance of risk group stratification derived from an independent Cox model constructed by using five conserved features from the hippocampus, parahippocampal gyrus and medial paracingulate gyrus in the PET model as predictors, and compared the Cox model constructed by the SUVR values of the corresponding brain regions and whole brain area. The results showed that high risk converters and low risk converters could be distinguished significantly in both models and the predictors found in our research outperform the SUVR value. In addition, our study also evaluated the changes of these crucial image markers at different cognitive stages in cross-section. Most features were significantly different between MCI-c and MCI-nc groups, or CI and HC groups. This provides strong evidence for using radiomic features to track the progress of high-risk individuals, which is very important for clinical purposes.

We draw attention to some limitations of this study. First, the sample size in our sub-cohort was relatively small, which could limit the statistical power and reproducibility of the results. In particular, the limited samples of the external test set (Cohort II, Huashan) may lead to the uncertainty in the C-index value of cohort II. We accept that further studies with larger and more heterogeneous external test groups are required to confirm our findings or refute. Second, this study lies in the lack of in-depth studies on the pathological mechanism, such as the pathological basis of crucial imaging markers, which could be further explored by combining genetic information as well as tau pathology in subsequent studies. Third, due to the lack of longitudinal data, the longitudinal changes of crucial image markers could not be explored.

5 Conclusions

In this study, we designed a workflow for radiomics-based predictive modelling analysis on PET images. Our results demonstrated that the combination of radiomic features extracted in the whole brain from PET images can more accurately predict MCI conversion, which had good stability and reliability, and can be used for disease stratification management. Moreover, the identified image biomarkers were significantly associated with cognitive ability and could reflect the differences at different cognitive stages. These preliminary tests demonstrated the potential of the RPM method as a clinical auxiliary tool to help MCI conversion prediction.

Declarations

Funding

This article was supported by grants from the National Natural Science Foundation of China (61603236 and 81830059, 81971641, 81671239 and 81361120393), Shanghai Municipal Science and Technology Major Project (No. 2017SHZDZX01, 2018SHZDZX03), and 111 Project (D20031). Data collection and sharing for this project were funded by the Alzheimers Disease Neuroimaging Initiative (ADNI; National Institutes of Health Grant U01 AG024904) and DODADNI (Department of Defense, award number W81XWH-12-2-0012). ADNI is funded by the National Institute of Aging and the National Institute of Biomedical Imaging and Bioengineering and through generous contributions from the following: AbbVie, Alzheimer's Association; Alzheimer's Drug Discovery Foundation; Araclon Biotech; BioClinica, Inc.; Biogen; Bristol-Myers Squibb Company; CereSpir, Inc.; Eisai, Inc.; Elan Pharmaceuticals,Inc.; Eli Lilly and Company; EuroImmun; F.Hoffmann-La Roche Ltd. and its affiliated company Genentech, Inc.; Fujirebio; GE Healthcare; IXICO Ltd.; Janssen Alzheimer Immunotherapy Research & Development, LLC.; Johnson &Johnson Pharmaceutical Research & Development LLC.; Lumosity; Lundbeck; Merck & Co., Inc.; Meso Scale Diagnostics,LLC.; NeuroRx Research; Neurotrack Technologies; Novartis Pharmaceuticals Corporation; Pfizer, Inc.; Piramal Imaging; Servier; Takeda Pharmaceutical Company; and Transition Therapeutics. The Canadian Institutes of Health Research is providing funds to support ADNI clinical sites in Canada. Private sector contributions are facilitated by the Foundation for the National Institutes of Health (www.fnih.org). The grantee organization is the Northern California Institute for Research and

Education, and the study is coordinated by the Alzheimer's Disease Cooperative Study at the University of California, San Diego,CA, USA. ADNI data are disseminated by the Laboratory for Neuro Imaging at the University of Southern California, CA, USA.

Data availability

Data is available under reasonable request to the corresponding author.

Code availability

The code is available under reasonable request to the corresponding author.

Ethics approval

Patient data used in this project was approved by institutional review boards of ADNI, Huashan, and Xuanwu hospital, and written informed consent was obtained from all participants or authorized representatives.

Consent to participate

Not applicable.

Consent for publication

Not applicable.

Conflict of Interest

The authors of this manuscript declare no relationships with any companies, whose products or services may be related to the subject matter of the article.

References

1. Huang K, Lin Y, Yang L, Wang Y, Cai S, Pang L et al. A multipredictor model to predict the conversion of mild cognitive impairment to Alzheimer's disease by using a predictive nomogram. Neuropsychopharmacology : official publication of the American College of Neuropsychopharmacology. 2020;45(2):358-66. doi:10.1038/s41386-019-0551-0.
2. Fan D-Y, Wang Y-J. Early Intervention in Alzheimer's Disease: How Early is Early Enough? neuroscience bulletin. 2020;36(2):195-7. doi:10.1007/s12264-019-00429-x.
3. Schneider JA, Arvanitakis Z, Leurgans SE, Bennett DA. The Neuropathology of Probable Alzheimer Disease and Mild Cognitive Impairment. Ann Neurol. 2009;66(2):200-8.
4. Petersen RC, Roberts RO, Knopman DS, Boeve BF, Geda YE, Ivnik RJ et al. Mild Cognitive Impairment Ten Years Later. Arch Neurol-Chicago. 2009;66(12):1447-55.

5. Blazhenets G, Ma Y, Sörensen A, Rücker G, Schiller F, Eidelberg D et al. Principal components analysis of brain metabolism predicts development of Alzheimer dementia. Journal of Nuclear Medicine. 2019;60(6):837-43.
6. Chaddad A, Desrosiers C, Hassan L, Tanougast C. Hippocampus and amygdala radiomic biomarkers for the study of autism spectrum disorder. BMC neuroscience. 2017;18(1):52.
7. Dubois B, Feldman HH, Jacova C, Hampel H, Molinuevo JL, Blennow K et al. Advancing research diagnostic criteria for Alzheimer's disease: the IWG-2 criteria. lancet neurology. 2014;13(6):614-29. doi:10.1016/S1474-4422(14)70090-0.
8. Jack CR, Bennett DA, Blennow K, Carrillo MC, Dunn B, Haeberlein SB et al. NIA-AA Research Framework: Toward a biological definition of Alzheimer's disease. alzheimers & dementia. 2018;14(4):535-62. doi:10.1016/J.JALZ.2018.02.018.
9. Wang M, Jiang J, Yan Z, Alberts I, Ge J, Zhang H et al. Individual brain metabolic connectome indicator based on Kullback-Leibler Divergence Similarity Estimation predicts progression from mild cognitive impairment to Alzheimer's dementia. Eur J Nucl Med Mol Imaging. 2020;47(12):2753-64. doi:10.1007/s00259-020-04814-x.
10. Zhou H, Jiang J, Lu J, Wang M, Zhang H, Zuo C. Dual-Model Radiomic Biomarkers Predict Development of Mild Cognitive Impairment Progression to Alzheimer's Disease. Front Neurosci. 2018;12:1045. doi:10.3389/fnins.2018.01045.
11. Petersen RC, Lundt ES, Therneau TM, Weigand SD, Knopman DS, Mielke MM et al. Predicting Progression to Mild Cognitive Impairment. Annals of neurology. 2019;85(1):155-60. doi:10.1002/ana.25388.
12. Rizzo S, Botta F, Raimondi S, Origgi D, Fanciullo C, Morganti AG et al. Radiomics: the facts and the challenges of image analysis. European radiology experimental. 2018;2(1):1-8.
13. Lambin P, Leijenaar RT, Deist TM, Peerlings J, De Jong EE, Van Timmeren J et al. Radiomics: the bridge between medical imaging and personalized medicine. Nature reviews Clinical oncology. 2017;14(12):749.
14. Feng Q, Chen Y, Liao Z, Jiang H, Mao D, Wang M et al. Corpus Callosum Radiomics-Based Classification Model in Alzheimer's Disease: A Case-Control Study. Frontiers in Neurology. 2018;9:618.
15. Li Y, Jiang J, Lu J, Jiang J, Zhang H, Zuo C. Radiomics: a novel feature extraction method for brain neuron degeneration disease using 18F-FDG PET imaging and its implementation for Alzheimer’s disease and mild cognitive impairment. therapeutic advances in neurological disorders. 2019;12. doi:10.1177/1756286419838682.
16. Zhao K, Ding Y, Han Y, Fan Y, Alexander-Bloch AF, Han T et al. Independent and reproducible hippocampal radiomic biomarkers for multisite Alzheimer’s disease: diagnosis, longitudinal progress and biological basis. chinese science bulletin. 2020. doi:10.1016/J.SCIB.2020.04.003.
17. Feng F, Wang P, Zhao K, Zhou B, Yao H, Meng Q et al. Radiomic features of hippocampal subregions in Alzheimer’s disease and amnestic mild cognitive impairment. Frontiers in Aging Neuroscience.

2018;10.

18. Feng Q, Wang M, Song Q, Wu Z, Jiang H, Pang P et al. Correlation Between Hippocampus MRI Radiomic Features and Resting-State Intrahippocampal Functional Connectivity in Alzheimer's Disease. Frontiers in neuroscience. 2019;13:435-. doi:10.3389/fnins.2019.00435.
19. Zhou H, Jiang J, Lu J, Wang M, Zhang H, Zuo C et al. Dual-model radiomic biomarkers predict development of mild cognitive impairment progression to Alzheimer’s disease. Frontiers in neuroscience. 2019;12:1045.
20. Jessen F, Amariglio RE, Van Boxtel M, Breteler M, Ceccaldi M, Chételat G et al. A conceptual framework for research on subjective cognitive decline in preclinical Alzheimer's disease. Alzheimer's & dementia. 2014;10(6):844-52.
21. Feng Q, Song Q, Wang M, Pang P, Liao Z, Jiang H et al. Hippocampus radiomic biomarkers for the diagnosis of amnestic mild cognitive impairment: A machine learning method. Frontiers in Aging Neuroscience. 2019;11:323.
22. Simon N, Friedman J, Hastie T, Tibshirani R. Regularization paths for Cox’s proportional hazards model via coordinate descent. Journal of statistical software. 2011;39(5):1.
23. Friedman J, Hastie T, Tibshirani R. Regularization paths for generalized linear models via coordinate descent. Journal of statistical software. 2010;33(1):1.
24. Therneau TM, Grambsch PM. Modeling survival data: extending the Cox model. Springer Science & Business Media; 2013.
25. Liu K, Chen K, Yao L, Guo X. Prediction of mild cognitive impairment conversion using a combination of independent component analysis and the Cox model. Frontiers in human neuroscience. 2017;11:33.
26. Mosconi L, Berti V, Glodzik L, Pupi A, Leon MJD. Pre-Clinical Detection of Alzheimer's Disease Using FDG-PET, with or without Amyloid Imaging. Journal of Alzheimers Disease. 2010;20(3):843-54.
27. Arbizu J, Festari C, Altomare D, Walker Z, Bouwman F, Rivolta J et al. Clinical utility of FDG-PET for the clinical diagnosis in MCI. European journal of nuclear medicine and molecular imaging. 2018;45(9):1497-508.
28. Christian S, Antonio C, Petronilla B, Gilardi MC, Aldo Q, Isabella C. Magnetic resonance imaging biomarkers for the early diagnosis of Alzheimer's disease: a machine learning approach. Frontiers in Neuroscience. 2015;9:307.
29. Tondelli M, Wilcock GK, Nichelli P, Jager CAD, Jenkinson M, Zamboni G. Structural MRI changes detectable up to ten years before clinical Alzheimer's disease. Neurobiology of Aging. 2012;33(4):825.e25-.e36.
30. Yang H, Xu H, Li Q, et al. Study of brain morphology change in Alzheimer's disease and amnestic mild cognitive impairment compared with normal controls. Gen Psychiatr. 2019;32(2):e100005. Published 2019 Apr 16. doi:10.1136/gpsych-2018-100005
31. B. Iordanova, D. Rosenbaum, D. Norman, M. Weiner, C. Studholme. MR Imaging Anatomy in Neurodegeneration: A Robust Volumetric Parcellation Method of the Frontal Lobe Gyri with

Quantitative Validation in Patients with Dementia. American Journal of Neuroradiology Sep 2006, 27 (8) 1747-1754;

Figures

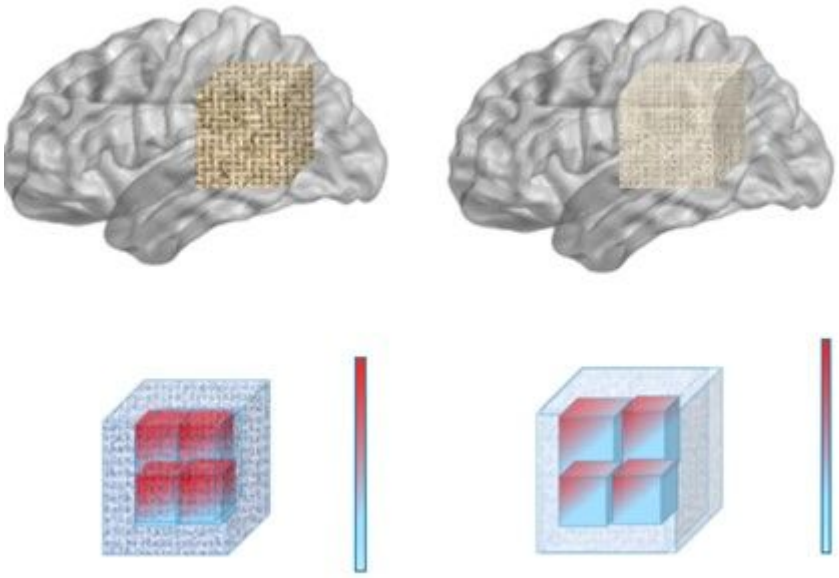

Figure 1

One case to demonstrate the importance of high dimensional characteristics.

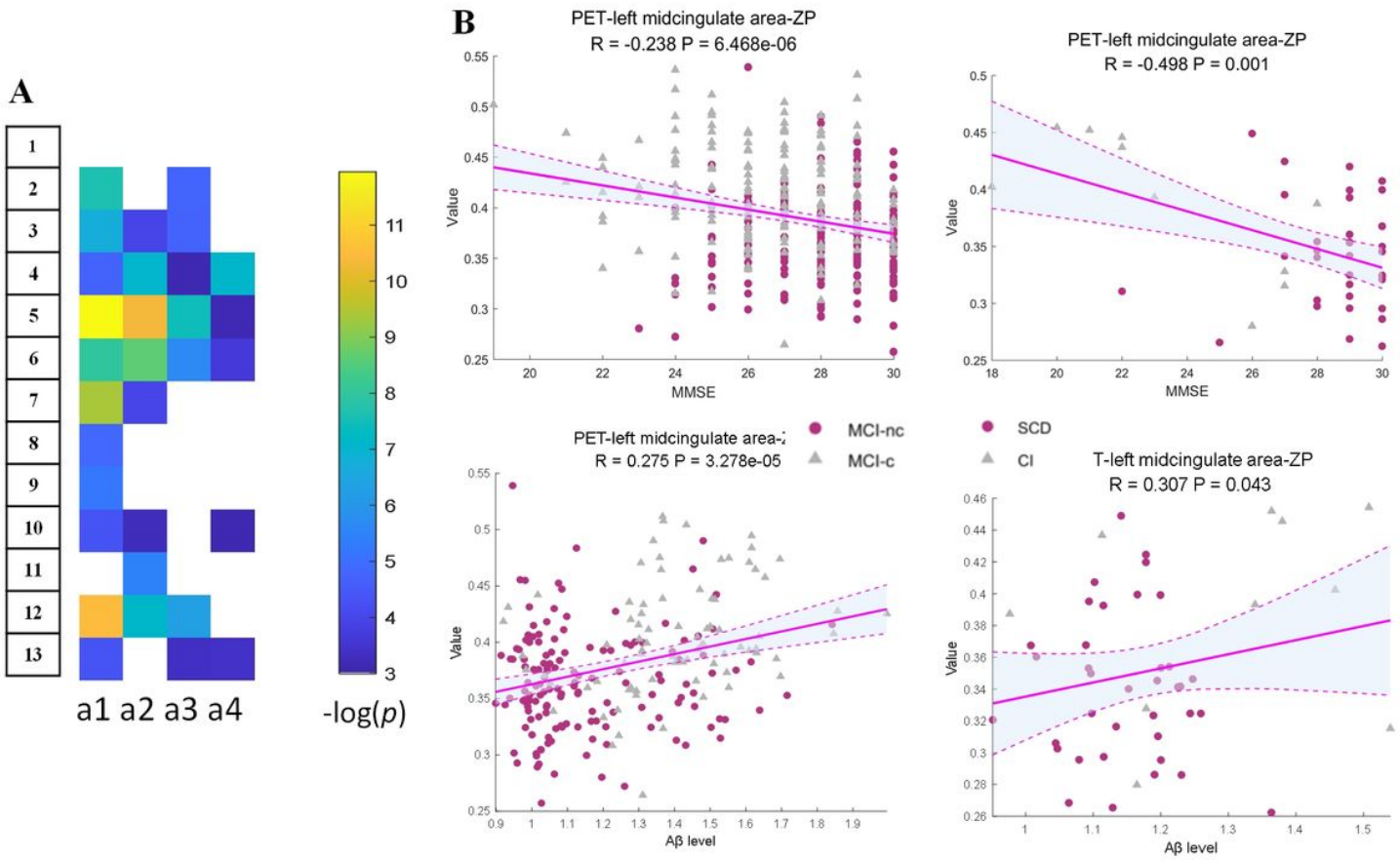

Figure 2

(A) Correlations between the MMSE score and Aβ scores with a subset of radiomics features. The values of the color bar reflected -log(P); a1: correlation with the MMSE scores in Cohort I by combining MCI-nc and MCI-c group; a2: correlation with the Aβ scores in Cohort I by combining MCI-nc and MCI-c group; a3: correlation with the MMSE scores in Cohort III by combining SCD and CI group; a4: correlation with the Aβ scores in Cohort III by combining SCD and CI group; the serial number indicated the feature order. (B) Scatterplots illustrated a significant correlation, this feature was zone percentage from the left midcingulate area.

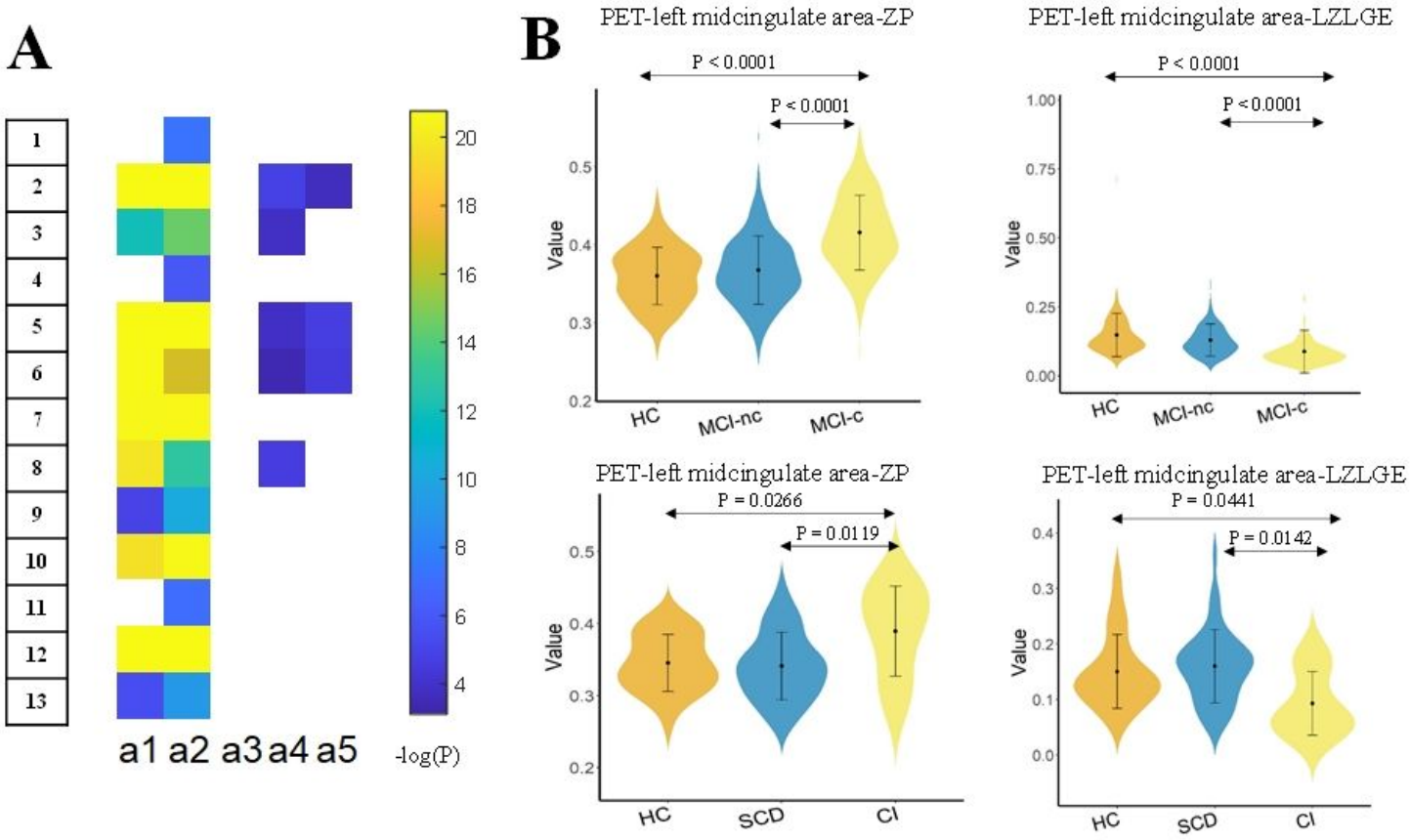

Figure 3

(A) Group differences of a subset of radiomic features at different cognitive stages. The values of the color bar reflected -log(P); a1: HC vs. MCI-nc in Cohort I. a2: HC vs. MCI-c in Cohort A; a3: MCI-nc vs. MCI-c in Cohort I; a4: HC vs. SCD in Cohort III; a5: HC vs. CI in Cohort III; a6: SCD vs. CI in Cohort III; the serial number indicated the feature order, corresponding to Tab.2. (B) Examples of feature distributions at different cognitive stages.

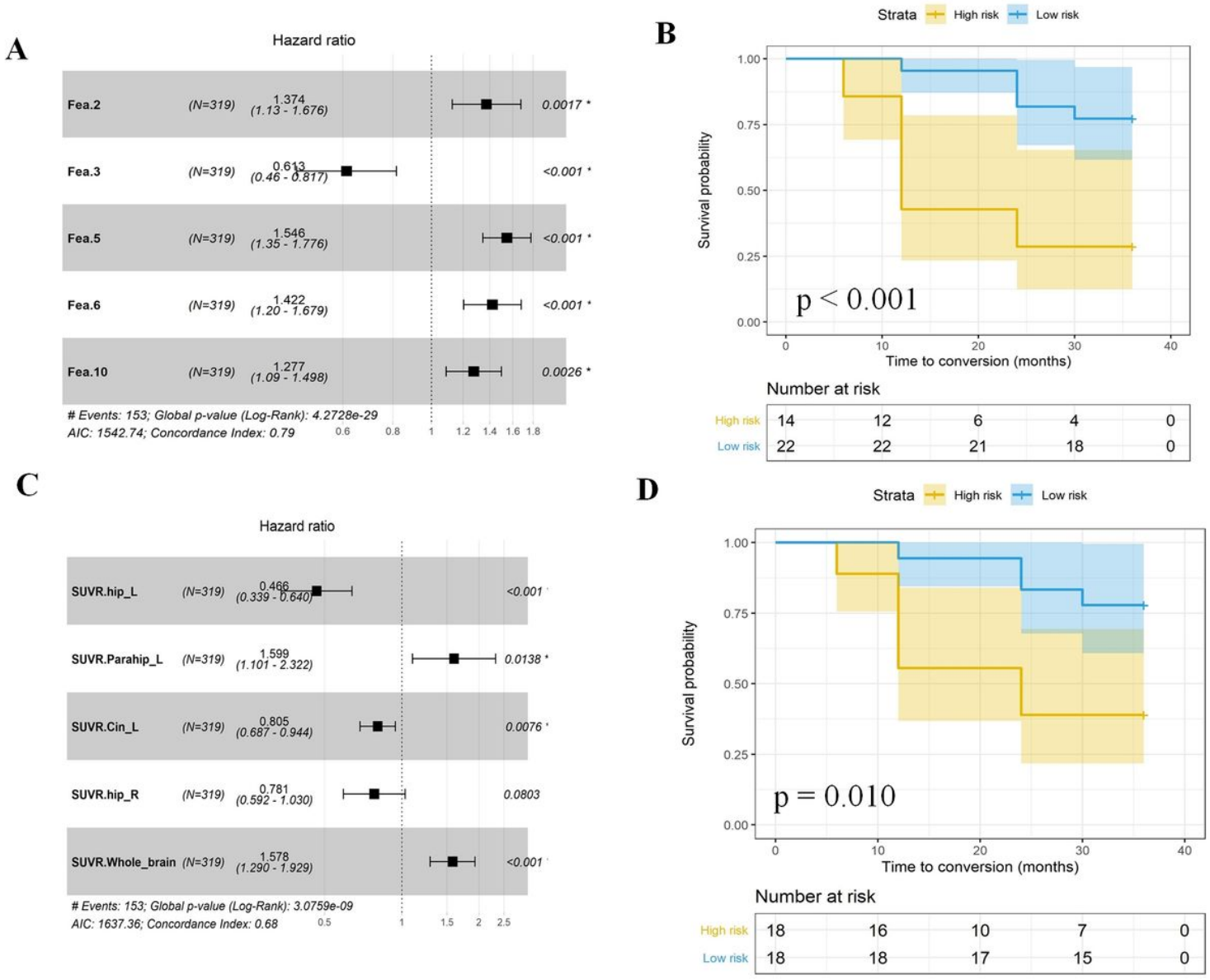

Figure 4

Hazard ratios for different predictors and Kaplan-Meier survival curves. (A) Hazard ratios for different feature predictors in the PET model, 5 features from the hippocampus, medial paracingulate gyrus and whole brain area in PET images as predictors, which were Fea.2, Fea.3, Fea.5, Fea.6 and Fea.10. (B) Risk stratification of test dataset in the PET model (log-rank test, P <0.001). (C) Hazard ratios for SUVR predictors in the PET model, 5 features from the hippocampus, medial paracingulate gyrus and whole brain area. (D) Risk stratification of test dataset in the PET model (log-rank test, P = 0.010).

Supplementary Files

This is a list of supplementary files associated with this preprint. Click to download.

- supp.docx